



LJMU Research Online

Aldeka, AB, Tziavos, NI, Gkantou, M, Dirar, S and Chan, AHC

Seismic design of non-structural components mounted on irregular reinforced concrete buildings

<http://researchonline.ljmu.ac.uk/id/eprint/16088/>

Article

Citation (please note it is advisable to refer to the publisher's version if you intend to cite from this work)

Aldeka, AB, Tziavos, NI, Gkantou, M, Dirar, S and Chan, AHC (2021) Seismic design of non-structural components mounted on irregular reinforced concrete buildings. Journal of Building Engineering, 46. ISSN 2352-7102

LJMU has developed **LJMU Research Online** for users to access the research output of the University more effectively. Copyright © and Moral Rights for the papers on this site are retained by the individual authors and/or other copyright owners. Users may download and/or print one copy of any article(s) in LJMU Research Online to facilitate their private study or for non-commercial research. You may not engage in further distribution of the material or use it for any profit-making activities or any commercial gain.

The version presented here may differ from the published version or from the version of the record. Please see the repository URL above for details on accessing the published version and note that access may require a subscription.

For more information please contact researchonline@ljmu.ac.uk

<http://researchonline.ljmu.ac.uk/>

Seismic design of non-structural components mounted on irregular reinforced concrete buildings

Ayad B. Aldeka¹, Nikolaos I. Tziavos², Michaela Gkantou³, Samir Dirar^{4*} and Andrew H.C. Chan⁵

¹Senior Lecturer, Nottingham Trent University, Nottingham, NG1 4FQ, UK

²Research Associate, University of Cambridge, Cambridge, CB3 0FA, UK

³Senior Lecturer, Liverpool John Moores University, Liverpool, L2 2QP, UK

⁴Associate Professor, University of Birmingham, Edgbaston, Birmingham, B15 2TT, UK

⁵Professor, University of Tasmania, Sandy Bay, TAS 7005, Australia

*Corresponding author, Email: s.m.o.h.dirar@bham.ac.uk

Abstract

The seismic response of non-structural components (NSCs) attached to irregular reinforced concrete (RC) multi-storey buildings is underestimated by current European design provisions. This paper presents a new design model for NSCs, accounting for the effect of torsion and seismic capacity of an irregular RC primary structure (P-structure). The proposed model is a modification of the current Eurocode 8 (EC8) model for the acceleration amplification factor of NSCs. It is based on the results of some 5000 nonlinear dynamic finite element analyses conducted on thirty-three building cases. The finite element analyses covered a wide range of parameters including plan layout, seismic capacity, fundamental vibration period, total height, floor rotation, ground type and eccentricity ratio. The proposed model has been demonstrated to be an improvement over EC8 model, especially for NSCs mounted on the flexible side and in tune with the fundamental vibration period of a P-structure.

Keywords: design; Eurocode 8; irregular buildings; non-structural components; torsion

30 **1. Introduction**

31 Non-structural components (NSCs) are members or devices attached to a building without
32 substantial contribution to its load resisting system. For instance, architectural elements such
33 as walls, partitions or façades are classified as NSCs along with mechanical and electrical
34 devices, also known as acceleration-sensitive components. In the aftermath of earthquake
35 events, it has been recognised that damage to NSCs could significantly affect occupants'
36 quality of life and have drastic consequences on the operation of residential and industrial
37 structures (McKevitt, 2004). Therefore, accurate prediction of the seismic performance of
38 NSCs using seismic codes such as Eurocode 8 (EC8) (2004), ASCE (2010), and UBC (2012)
39 is of utmost importance in order to ensure both safety and functionality.

40 Studies on the dynamic behaviour of architectural components attached to primary
41 structures (P-structures) have been reported by Yang and Huang (1993, 1998), Agrawal (1999),
42 Agrawal and Datta (1999a, 1999b), Mohammed *et al.* (2008), Johnson *et al.* (2016), Lim *et al.*
43 (2017), and Sousa and Monteiro (2018). However, our understanding of the behaviour of
44 acceleration-sensitive NSCs attached to irregular reinforced concrete (RC) P-structures is still
45 relatively limited. Lima and Martinelli (2019) examined the mechanical parameters governing
46 the performance of acceleration-sensitive NSCs. Upon performing a nonlinear dynamic study
47 on RC buildings, Petrone *et al.* (2015) found that EC8 (2004) underestimates the seismic
48 demands of light NSCs for a wide range of excitation frequencies. Focussing on irregular RC
49 multi-storey buildings, Aldeka *et al.* (2014a, 2014b, 2015) studied the response of acceleration-
50 sensitive NSCs attached along the heights of irregular P-structures by means of nonlinear
51 dynamic finite element analyses (FEA) and demonstrated that EC8 (2004) underestimates the
52 performance of NSCs. Mohsenian *et al.* (2019) investigated the seismic demand of non-
53 structural components and concluded that currently employed design codes may underestimate
54 the accelerations applied to NSCs by up to 80%. Based on published data, Filiatrault and
55 Sullivan (2014) emphasised the lack of accuracy when designing NSCs under seismic actions.
56 Similarly, Martinelli and Faella (2016) presented an overview of seismic code rules suggesting
57 that current design equations could not predict adequately the interaction between the P-
58 structures and NSCs. Most recently, Anajafi and Medina, (2018, 2019) examined the floor
59 spectra of instrumented buildings in order to evaluate the effects of torsional flexibility on the
60 seismic design of non-structural components. They concluded that significant torsional
61 response can result in increased NSCs seismic demand, particularly for NSCs at a floor

62 periphery and away from elements of the lateral-force resisting systems. Moreover, they
63 showed that parameters like floor diaphragm flexibility, vertical irregularity in mass and
64 stiffness, and seismic base isolation can affect NSCs acceleration demand. Surana et al. (2018)
65 studied the torsional effects of hill-side RC buildings with irregular configurations and
66 proposed spectral amplification functions that can take into account the effect of the buildings'
67 plan and elevation irregularities on the response of NSCs. In the absence of codified provisions
68 for hill-side buildings, they suggested that the proposed functions could be used for seismic
69 design of acceleration-sensitive NSCs for a given structure, ground motion response spectrum
70 and NSC location.

71 Aiming to address the gap in current seismic design codes, this paper presents a new design
72 expression that improves the predictions of the current EC8 (2004) model for the design of
73 acceleration-sensitive NSCs. It takes into consideration the maximum seismic capacity and the
74 torsional behaviour of P-structures. The new design model is calibrated and validated against
75 the results of some 5000 nonlinear dynamic FEA of NSCs attached to irregular RC buildings.
76 The design data are presented in Section 3. A proposal for modifying EC8 (2004) design model
77 for NSCs is presented in Section 4. The proposed model is assessed in Section 5 on the basis
78 of FEA results for an extensive range of P-structures.

79 **2. Research significance**

80 In seismic codification, acceleration amplification factors are used in the design of NSCs to
81 guarantee safe and functional designs. This approach ensures that NSCs of critical importance,
82 such as medical, electrical and mechanical equipment, are designed in such a way that they
83 remain fully functional under seismic actions in lifeline structures such as hospitals, power
84 plants, and factories. However, the design of acceleration-sensitive NSCs is currently
85 underestimated by design codes. Damage of such NSCs could pose risk to human life and result
86 in significant economic losses. Hence it is deemed essential that NSCs be designed to withstand
87 earthquake action without damage. This paper proposes a new model for the design of
88 acceleration-sensitive NSCs that takes into account the effect of the torsional response and the
89 maximum seismic capacity of P-structures.

90

91 3. Design data

92 This section gives an overview of the numerical results which formed the basis for the
93 development, calibration and validation of a new seismic design model for NSCs. For this
94 purpose, a comprehensive data-set comprising 5194 nonlinear dynamic FEA was utilised. The
95 numerical models cover a series of geometries and parameters, which are presented in Section
96 3.1. The key results along with the main modelling considerations are briefly described in
97 Section 3.2. Further details on the development of the FE models and numerical
98 implementation can be found in Aldeka *et al.* (2014a, 2014b, 2015).

99 3.1. Geometries and parameters

100 The main aim of the numerical investigations was to quantify the response of NSCs under
101 seismic actions. Therefore, a wide range of buildings with varying heights, ground types and
102 eccentricity ratios were considered from the authors' previous studies (Aldeka *et al.*, 2014a;
103 2014b; 2015), resulting in a total of thirty-three irregular RC P-structures. The NSCs
104 considered were elastic, lightweight, acceleration-sensitive components, such as mechanical
105 equipment found in industrial buildings, electrical components found in commercial buildings
106 or medical equipment found in healthcare centres. The investigated P-structures were
107 categorised into four groups of buildings.

108 Group 1 (G1) comprised four irregular three-storey RC P-structures with a common plan layout
109 and a total height of 9 m. G1-1 was designed to resist vertical loads only, whereas G1-2 and
110 G1-3 were designed according to EC8 (2004). Type 1 spectrum for ground type C and a design
111 ground acceleration (a_g) of 0.15 g and 0.25 g, respectively was employed. The values of the
112 over-strength factor (γ_{Rd}) for G1-2 and G1-3 did not satisfy the global and local ductility
113 requirements recommended by EC8 (2004), hence, G1-4 which conforms to EC8 (2004)
114 Ductility Class M requirements was also included in the group. The concrete class was C25/30
115 and the steel reinforcement was Grade 400 for all G1 buildings except for G1-1 which had steel
116 reinforcement with a nominal yield strength of 459 MPa (Rozman and Fajfar 2009).

117 Group 2 (G2) comprised five irregular RC P-structures with the same plan layout and storey
118 height (i.e., 3 m) as G1 buildings. In this case the total height was modified, resulting in 5-, 7,
119 10-, 13- and 15- storey buildings designated as G2-1, G2-2, G2-3, G2-4 and G2-5. The group
120 was designed according to EC8 (2004) Ductility Class M requirements using Type 1 spectrum

121 for ground type C, a_g value of 0.25 g and a behaviour factor (q) of 3.45. Concrete Class
 122 C25/30 and steel reinforcement Class C S500 were used.

123 In Group 3 (G3), the ground type (A, B, D, E) was varied as per EC8 (2004) for four different
 124 heights. Four irregular RC P-structures (G3-1, G3-2, G3-3 and G3-4) with the same plan layout
 125 as G1-1 and four different heights ranging from 9 to 45 m were examined resulting in a total
 126 of 16 RC P-structures. An elastic response spectrum consistent with Type 1 was applied. The
 127 behaviour factor was taken equal to 3.45 and the design acceleration for Type A ground was
 128 taken equal to 0.25 g.

129 Finally, in Group 4 (G4), the effect of eccentricity ratio (R) on the response of eight three-
 130 storey RC buildings was assessed. The investigated P-structures (G4-1 to G4-8) had R values
 131 of 0.0, 0.026, 0.060, 0.098, 0.143, 0.205, 0.284, and 0.372, respectively, in two perpendicular
 132 horizontal directions (i.e. $R_x = R_y$). As shown in Fig. 1(b), the P-structures had a single bay of
 133 5.5 m in both X and Y directions and square column cross-sections. The design of G4 P-
 134 structures was carried out according to Eurocodes EC1 (2002), EC2 (2004), and EC8 (2004).

135 The plan layouts of the modelled buildings are shown in Fig. 1, where the eccentricities
 136 between their centres of rigidity (CR) and centres of mass (CM) are also shown. In this paper,
 137 the eccentricity ratio in a given direction is defined as the static eccentricity in that direction
 138 divided by the elasticity radius. Initially, the CM coordinates (g_x, g_y) were calculated as follows:

$$g_x = \frac{\sum_{i=1}^N (w_i \cdot x)}{\sum_{i=1}^N w_i} \quad (1)$$

$$g_y = \frac{\sum_{i=1}^N (w_i \cdot y)}{\sum_{i=1}^N w_i} \quad (2)$$

139 where N is the number of the structural members, w_i is the weight of a structural member,
 140 and x and y are the member coordinates. Subsequently, the CR coordinates (l_x, l_y) were
 141 calculated as follows using the lateral stiffness of the structural members, K_x and K_y :

$$l_x = \frac{\sum (K_y \cdot x)}{\sum K_y} \quad (3)$$

$$l_y = \frac{\sum (K_x \cdot y)}{\sum K_x} \quad (4)$$

142 K_x and K_y were calculated using MIDAS Gen ver. 2.1 (2012). The reader is referred to

143 MIDAS Gen (2012) Analysis Manual for further details. The static eccentricity in a given
 144 direction was calculated as follows:

$$e_x = |\ell_x - g_x| \quad (5)$$

$$e_y = |\ell_y - g_y| \quad (6)$$

145 The torsional stiffness, K_R of a structure about its centre of rigidity, CR is given by:

$$K_R = \sum (K_x \cdot \bar{Y}^2) + (K_y \cdot \bar{X}^2) \quad (7)$$

146 where \bar{X} and \bar{Y} may be calculated as:

$$\bar{X} = x - \ell_x \quad (8)$$

$$\bar{Y} = y - \ell_y \quad (9)$$

147 The radii of elasticity in the two horizontal directions (r_{ex} and r_{ey}) were calculated as foll
 148 ows:

$$r_{ex} = \sqrt{\frac{K_R}{\sum K_x}} \quad (10)$$

$$r_{ey} = \sqrt{\frac{K_R}{\sum K_y}} \quad (11)$$

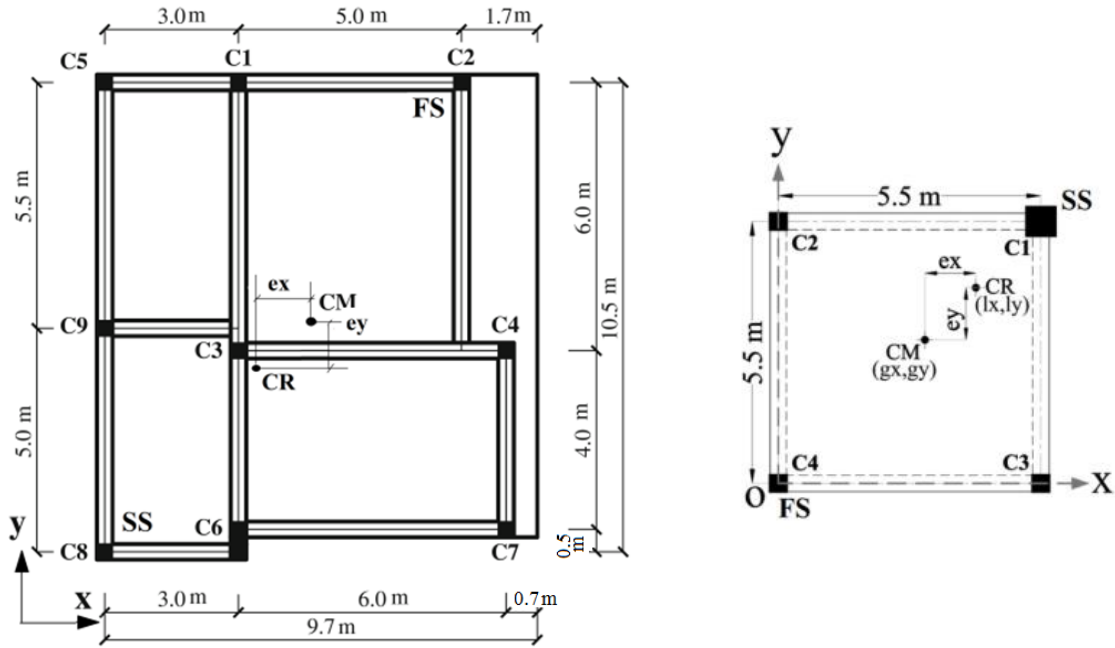
149 Finally, the eccentricity ratios R_{ex} and R_{ey} in X and Y directions, respectively, were calc
 150 ulated as follow:

$$R_{ex} = e_y / r_{ex} \quad (12)$$

$$R_{ey} = e_x / r_{ey} \quad (13)$$

151 It should be noted that the eccentricity ratios reported in this paper correspond mainly to the
 152 top floors of the P-structures. For the analysis and interpretation of the numerical results, the
 153 following key characteristic design parameters were evaluated for each group: a) the
 154 fundamental vibration periods of the P-structures and the NSCs, b) the maximum seismic
 155 capacities of the P-structures and c) the top-floor rotations. A summary of the characteristic
 156 design parameters for each model is given in Table 1.

157



a) Groups 1, 2, 3 (G1, G2, G3)

b) Group 4 (G4)

Fig. 1: Plan layouts of modelled P-structures (Aldeka *et al.*, 2014a, 2014b, 2015)

158 3.2. Modelling considerations and key results

159 For the thirty-three cases (Aldeka *et al.*, 2014a, 2014b, 2015) presented in Section 3.1, the
 160 finite element program MIDAS Gen ver. 2.1 (2012) was employed to conduct nonlinear
 161 dynamic analyses. The P-structures were modelled using distributed inelastic fibre elements.
 162 The concrete behaviour was defined using the confined and unconfined concrete models
 163 proposed by Mander *et al.* (1988) whereas the steel reinforcement was modelled using the
 164 analytical model by Menegotto and Pinto (1973) for cyclic loads. Natural and artificial
 165 earthquake records comprising 70 accelerograms were adopted for the selected analyses.
 166 REXEL software (Iervolino *et al.*, 2010) from the European Strong-motion Database (ESD)
 167 was used to obtain the natural records. SIMQKE code (Gelfi, 2007) was used to generate
 168 artificial records. A NSC was modelled as a fixed vertical cantilever with a lumped mass at its
 169 free end. This approach has been widely adopted in previous studies (see e.g., Sackman and
 170 Kelly, 1979; Yang and Huang, 1998; Agrawal, 1999; Mohammed *et al.* 2008; Chauduri and
 171 Villaverde, 2008; Opropeza *et al.*, 2010). The vibration period (T_C) of the NSC matched one
 172 of the first three vibration periods (T_1 , T_2 , or T_3) of the P-structure. Based on the
 173 recommendation by Graves and Morante (2006), a damping ratio of 3% was employed for the
 174 NSCs but further research is recommended to investigate the effect of NSC damping ratio on

175 the accuracy of design model predictions. For further details on the validation of the nonlinear
176 dynamic FE model, the reader is referred to Aldeka *et al.* (2014a). In total, 5194 nonlinear
177 dynamic FEA were carried out and form the basis of the calibration and validation of the new
178 design model presented in this paper.

179 In Table 1, key results are listed along with the labelling used in the references, the updated
180 notation applied in this paper, and the ground type for each case. In particular, T_c , the
181 fundamental vibration period of the NSCs; and T_1 , T_2 , and T_3 ; the first three vibration periods
182 of the P-structures, are reported. T_1 and T_2 refer to the translational mode periods whereas T_3
183 refers to the torsional mode period. For Groups 1 and 4, NSCs with fundamental vibration
184 periods similar to the first three vibration periods of the P-structures were considered. In Group
185 2, T_1 and T_2 were approximately equal hence NSCs with fundamental vibration periods similar
186 to T_1 and T_3 were considered. In Group 3, NSCs with $T_c = T_1$ were considered.

187 The elastic and maximum (F_{SC}) seismic capacities of the P-structures in [g] are also given
188 in Table 1. The elastic and maximum seismic capacities were calculated using the extended N2
189 procedure. This is a simplified nonlinear method for the seismic analysis of plan-asymmetric
190 structures. In the extended N2 procedure, the results of a three-dimensional nonlinear static
191 (push-over) analysis are combined with the results of a modal analysis of a two-dimensional
192 model. The extended N2 method has been demonstrated to provide reasonable predictions of
193 the torsional influences in asymmetric structures (Fajfar, 2002; Fajfar et al., 2005a; Kreslind
194 and Fajfar, 2013; Stefano and Pintucchi, 2010).

195

Table 1: Key results from collated data.

Labelling of Reference	Notation herein	Ground type	Fund. period, T [s]	Elastic Capacity factor [g]	Max. Capacity factor [g] F_{SC}	Top rotation, θ [rad]	F_T mean Eq. (14)	T_C			
								T_1	T_2	T_3	
Group 1 (Aldeka <i>et al.</i> , 2014a)	Test	G1-1	--	0.82	0.070	0.26	0.0084	1.36	0.82	0.73	0.65
	Test 0.15	G1-2	C	0.82	0.100	0.46	0.0084	1.36	0.82	0.73	0.65
	Test 0.25	G1-3	C	0.82	0.120	0.51	0.0077	1.33	0.82	0.73	0.65
	EC8 M	G1-4	C	0.55	0.135	0.76	0.0038	1.16	0.55	0.52	0.42
Group 2 (Aldeka <i>et al.</i> , 2014a)	EC8 M5	G2-1	C	0.66	0.160	0.74	0.0045	1.19	0.66	-	0.51
	EC8 M7	G2-2	C	0.84	0.160	0.69	0.0059	1.26	0.84	-	0.66
	EC8 M10	G2-3	C	1.17	0.160	0.63	0.0090	1.39	1.17	-	0.92
	EC8 M13	G2-4	C	1.29	0.170	0.58	0.0106	1.46	1.29	-	1.02
	EC8 M15	G2-5	C	1.39	0.170	0.58	0.0117	1.51	1.39	-	1.12
Group 3 (Aldeka <i>et al.</i> , 2014b)	EC8 M3	G3-1A	A	0.620	0.120	0.69	0.0052	1.23	0.62	-	-
		G3-1B	B	0.590	0.131	0.72	0.0046	1.20	0.59	-	-
		G3-1D	D	0.470	0.149	0.83	0.0024	1.10	0.47	-	-
		G3-1E	E	0.520	0.143	0.79	0.0029	1.13	0.52	-	-
		G3-2A	A	0.750	0.142	0.64	0.0067	1.29	0.75	-	-
	EC8 M5	G3-2B	B	0.710	0.156	0.68	0.0057	1.25	0.71	-	-
		G3-2D	D	0.610	0.179	0.78	0.0032	1.14	0.61	-	-
		G3-2E	E	0.660	0.160	0.74	0.0047	1.20	0.66	-	-
	EC8 M10	G3-3A	A	1.250	0.135	0.57	0.0102	1.44	1.25	-	-
		G3-3B	B	1.220	0.150	0.59	0.0096	1.42	1.22	-	-
		G3-3D	D	1.080	0.178	0.70	0.0057	1.25	1.08	-	-
		G3-3E	E	1.170	0.160	0.63	0.0091	1.39	1.17	-	-
	EC8 M15	G3-4A	A	1.500	0.148	0.50	0.0163	1.71	1.50	-	-
		G3-4B	B	1.450	0.168	0.54	0.0140	1.61	1.45	-	-
		G3-4D	D	1.280	0.192	0.64	0.0081	1.35	1.28	-	-
G3-4E		E	1.390	0.170	0.58	0.0117	1.51	1.39	-	-	
Group 4 (Aldeka <i>et al.</i> , 2015)	Reference ($R_x=R_y=0.000$)	G4-1	C	0.385	0.15	0.57	0.0000	1.00	0.385	0.379	0.261
	Modified 1 ($R_x=R_y=0.026$)	G4-2	C	0.385	0.14	0.57	0.0003	1.01	0.385	0.379	0.261
	Modified 2 ($R_x=R_y=0.060$)	G4-3	C	0.385	0.14	0.56	0.0007	1.03	0.385	0.379	0.261
	Modified 3 ($R_x=R_y=0.098$)	G4-4	C	0.385	0.14	0.55	0.0013	1.06	0.385	0.379	0.261
	Modified 4 ($R_x=R_y=0.143$)	G4-5	C	0.385	0.14	0.55	0.0022	1.10	0.385	0.379	0.261
	Modified 5 ($R_x=R_y=0.205$)	G4-6	C	0.385	0.15	0.55	0.0038	1.16	0.385	0.379	0.261
	Modified 6 ($R_x=R_y=0.284$)	G4-7	C	0.385	0.15	0.54	0.0072	1.31	0.385	0.379	0.261
	Modified 7 ($R_x=R_y=0.372$)	G4-8	C	0.385	0.15	0.54	0.0114	1.49	0.385	0.379	0.261

199 4. Proposed model for the seismic design of NSCs

200 Aldeka *et al.* (2014a, 2014b, 2015) demonstrated that, at the design PGA of the P-structures,
201 EC8 (2004) underestimates the acceleration response of NSCs with T_C equal to T_I and attached
202 to the flexible sides of the top floors by about 35%. Similarly, an underestimation of about 52%
203 was observed at the PGA values corresponding to the maximum seismic capacities of the P-
204 structures. This is attributed to the fact that EC8 (2004) does not explicitly account for the
205 increase in NSCs accelerations caused by the torsional behaviour of the P-structures.

206 In Eq. (14) the relationship between the torsional amplification factor for NSCs
207 accelerations (F_T) and the rotation (θ) of the top floor is given, as presented by Aldeka *et al.*
208 (2014a), for NSCs with T_C equal to T_I . The torsional amplification factor (F_T) is defined as the
209 ratio of the peak component acceleration at the flexible side ($PCA_{xy,FS}$) to the corresponding
210 value at the centre of the rigidity ($PCA_{xy,CR}$). PCA_{xy} is computed as the square root of the sum
211 of the squares of PCA_x and PCA_y . PCA_x and PCA_y are the peak component acceleration (PCA)
212 values in the horizontal x and y directions, respectively. Eq. (14) was used to quantify F_T for
213 the thirty-three cases reported in Section 3.1 and the results are presented in Table 1.

$$F_T = 43.3\theta + 1.0 \quad (14)$$

214 Eq. (14) calculates F_T as a function of θ only. However, in the proposed design model (see Eq.
215 (17)), a linear variation of F_T along the height of a P-structure is considered by multiplying F_T
216 with z/H (i.e., the relative position of NSCs).

217
218 Even though the behaviour of NSCs can be influenced by the P-structure torsional response,
219 this is currently not considered by EC8 (2004) provisions. In particular, Section 4.3.5.2 of EC8
220 (2004) suggests Eq. (15) for calculating the NSC acceleration amplification factor:

$$\frac{S_a}{\alpha S} = \left[\frac{3[1 + (z/H)]}{1 + [1 - (T_C/T_1)]^2} - 0.5 \right] \quad (15)$$

221 where

222 S_a : seismic coefficient applicable to NSC

223 α : the ratio of the design ground acceleration on type A ground to the acceleration of gravity

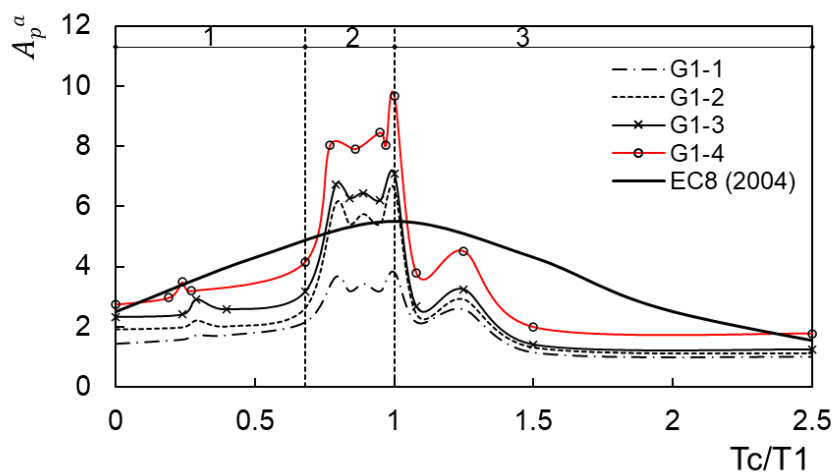
224 S : soil factor (S is taken as 1.0, 1.2, 1.15, 1.35, or 1.40 for ground types A, B, C, D, or E,
225 respectively, considering Type 1 elastic response spectrum of EC8)

226 T_C : fundamental vibration period of the NSC

227 T_I : fundamental vibration period of the P-structure (in the examined direction)

228 z : height of the NSC above the level of application of the seismic action and
 229 H : building height measured from the level of application of the seismic action.

230 Utilising the FE results of the NSCs attached to Group 1 buildings, the underconservative
 231 nature of Eq. (15) is demonstrated in Fig. 2, which shows the variations of the acceleration
 232 amplification factor (A_p^a) with T_c/T_1 . The acceleration amplification factor (A_p^a) is defined
 233 as PC_{Axy}/PGA for the NSCs attached to the flexible sides of the top floors. Fig. 2 also
 234 compares the results of the NSCs attached to Group 1 buildings (G1-1, G1-2, G1-3 and G1-4)
 235 with the predictions of Eq. (15). Although G1-1, G1-2 and G1-3 had the same fundamental
 236 periods (see Table 1), their NSCs acceleration response increased with the maximum seismic
 237 capacities of P-structures (F_{sc}). Eq. (15) conservatively predicted the response of the NSCs
 238 attached to G1-1, which was designed for gravity loads only. Moreover, as also shown in Fig.
 239 2 and explained in Aldeka *et al.* (2014a, 2014b, 2015), the response of NSCs with $T_c \approx 0s$ (i.e.,
 240 rigid NSCs) could be adequately predicted by Eq. (15). However, as can also be observed in
 241 Fig. 2, Eq. (15) significantly underestimated the amplification factors for NSCs with T_c/T_1
 242 values in the range of 0.68 to 1.0. Similar trends to those presented in Fig. 2 were reported by
 243 Aldeka *et al.* (2014a, 2014b, 2015). Hence evaluating the NSCs behaviour using only the
 244 fundamental vibration period can lead to inaccurate estimations. This is more pronounced in
 245 Zone 2 than in Zones 1 and 3 (see Fig. 2), where Zones 1, 2 and 3 correspond to $0 \leq T_c/T_1 \leq$
 246 0.68 , $0.68 \leq T_c/T_1 \leq 1.0$, and $1.0 \leq T_c/T_1 \leq 2.5$, respectively. Hence, Eq. (15) is hereinafter
 247 modified in such a way that it better predicts the acceleration response of NSCs attached to
 248 irregular RC P-structures.



249
 250 Fig. 2: Acceleration amplification factor (A_p^a) for varying NSC to P-structure period ratio
 251 (T_c/T_1)

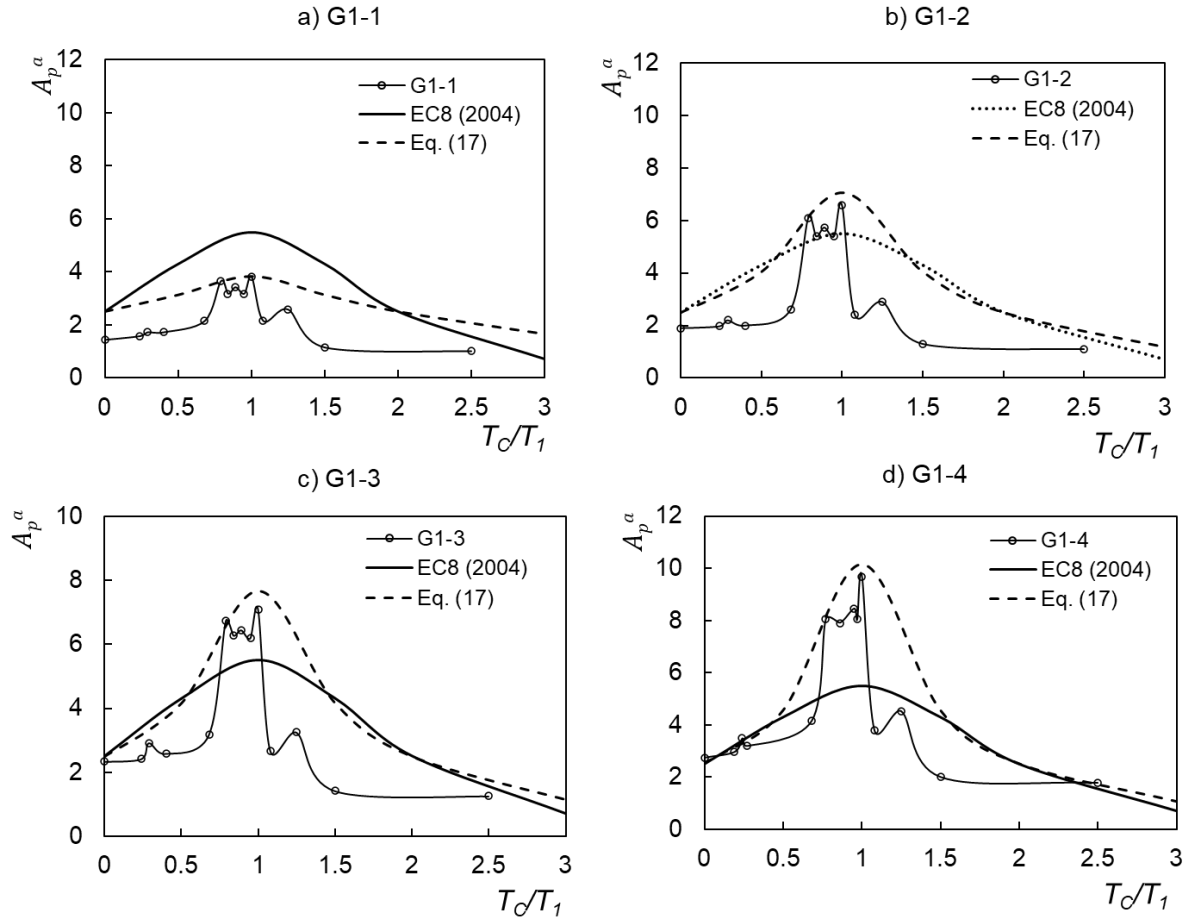
252 In order to take into consideration the torsional amplification factor (F_T) along with the
 253 maximum seismic capacity (F_{SC}) of the P-structure, Eq. (15) is modified based on statistical
 254 calibration of the FE results of Group 1 buildings. The parameters F_T and F'_{SC} are
 255 incorporated into Eq. (16) in such a way that its predictions are in agreement with the FE results
 256 of the NSCs in Zone 2 (see Fig. 2).

$$\frac{S_a}{\alpha S} = \left[\frac{6[1 + (z/H)]F_T F'_{SC}}{1 + [1 - (T_c/T_1)]^2} - 0.5 \right] \quad (16)$$

257 The dimensionless parameter F'_{SC} is the maximum seismic capacity (F_{SC}), as defined in
 258 Table 1, divided by the acceleration of gravity [g]. In order to avoid overestimating the
 259 acceleration response of rigid NSCs (i.e., with $T_c = 0$ s), which are adequately predicted by Eq.
 260 (15) as can be seen in Fig. 2, Eq. (16) is further modified by multiplying the term $(1 - (T_c/T_1))^2$
 261 with the term $(4F_T F'_{SC} - 1)$. This ensures an acceleration amplification value of 2.5 for rigid
 262 NSCs (i.e., similar to that predicted by Eq. (15) as can be seen in Fig. 3). Eq. (16) is further
 263 calibrated on the basis of the FE results of the NSCs that are out-of-tune with the first three
 264 vibration periods of the P-structures by applying an exponent of 3/5 to the term $(1 - (T_c/T_1))^2$.
 265 Hence, Eq. (16) can be re-written as follows:

$$\frac{S_a}{\alpha S} = \left[\frac{6[1 + (z/H)]F_T F'_{SC}}{1 + (4F_T F'_{SC} - 1)[1 - (T_c/T_1)]^2)^{3/5}} - 0.5 \right] \quad (17)$$

266 Figs. 3(a) to 3(d) present the variations of the acceleration amplification factor (A_p^a) with
 267 T_c/T_1 for Group 1 buildings. The FE results are compared with the predictions of EC8 (2004)
 268 (i.e., Eq. (15)) and Eq. (17). It is shown that Eq. (17) provides improved estimations for the
 269 NSCs attached to the top floors of G1 buildings. In addition, as shown in Fig. 3(a), Eq. (17)
 270 correctly predicts lower acceleration response than EC8 (2004) for the case of the NSCs
 271 attached to building G1-1. This better prediction is made possible by Eq. (17) taking into
 272 consideration the relatively low maximum seismic capacity of building G1-1 (0.26 g). Overall,
 273 Eq. (17) provides better estimations compared with EC8 (2004) (i.e., Eq. (15)) for the NSCs
 274 attached to Group 1 buildings, demonstrating adequate calibration.



275

276 Fig. 3: Acceleration amplification factor (A_p^α) versus NSC to P-structure period ratio (T_C/T_1)

277 **5. Assessment of the proposed design model**

278 In this section, the assessment of the proposed design model (i.e., Eq. (17)) is presented.
 279 The proposed design model differs from current EC8 (2004) design provisions (i.e., Eq. (15))
 280 in that Eq. (17) takes into consideration the torsional behaviour and the maximum seismic
 281 capacity of the P-structure. Thus, in order to use Eq. (17), the values of F_T and F_{SC} are required.
 282 For a given P-structure, a pushover analysis gives F_{SC} together with the rotation (θ) of the top
 283 floor. Once θ is known, Eq. (14) may be used to calculate F_T .

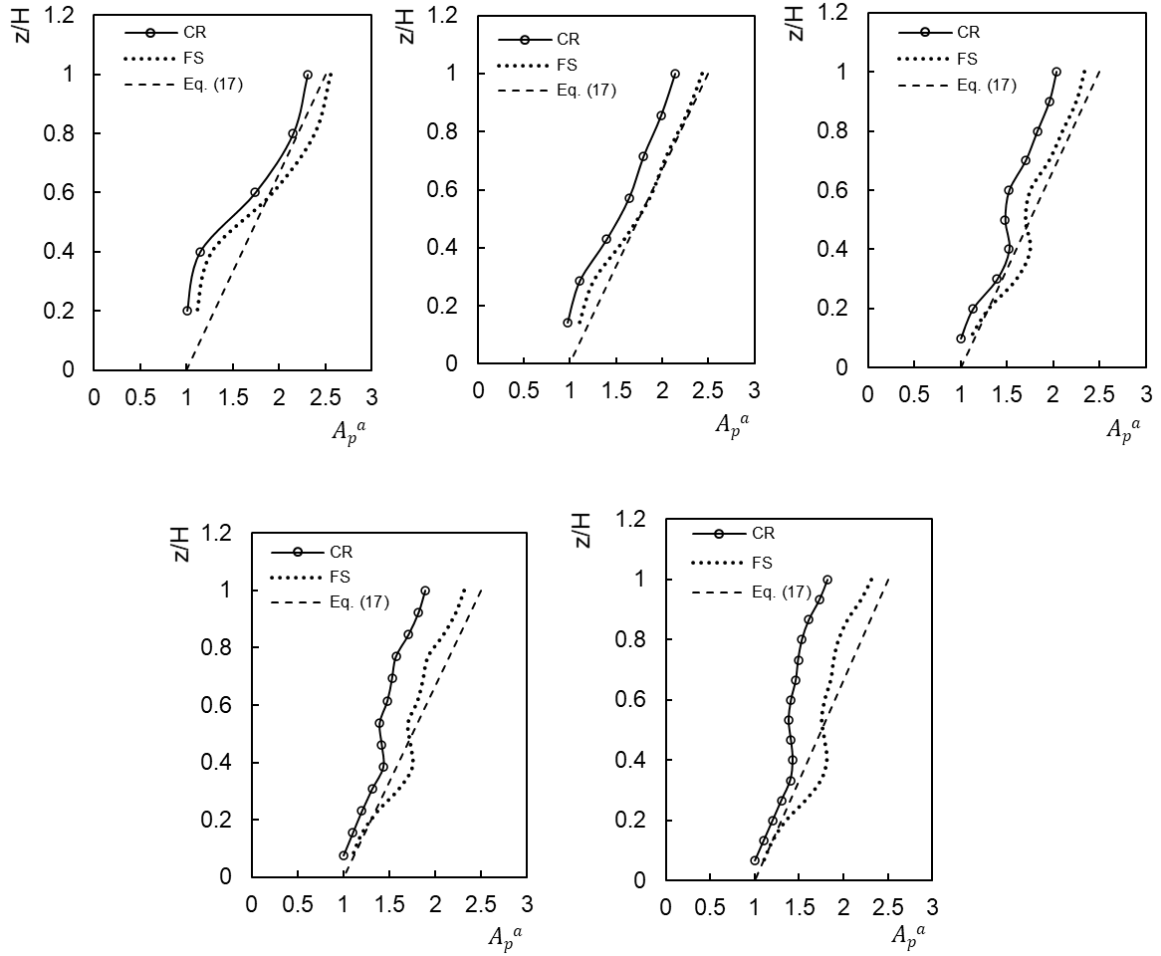
284 In the following sections, the accuracy of the proposed design model is assessed using the
 285 FE results of the NSCs attached to the buildings in Groups 2, 3 and 4. The FE results of Group
 286 1 buildings were not used in the assessment because they were used to calibrate the design
 287 model.

288

289 **5.1. Effect of P-structure height**

290 In Group 2, the focus was on the effect of P-structure height on the response of NSCs attached
291 to irregular RC buildings. The suitability of the proposed design model (i.e., Eq. (17)) for
292 predicting the seismic response of the NSCs attached to G2 buildings is assessed in this section.
293 Figs. 4-6 compare the predictions of Eq. (17) with the FE-predicted acceleration amplification
294 factors (A_p^a) for the NSCs at the centre of rigidity (CR) and on the flexible side (FS). The
295 results are presented as a function of z/H , where z and H are as defined in Section 4.

296 For rigid NSCs, Fig. 4 shows that the proposed model yields safe predictions for A_p^a values at
297 the centre of rigidity. The model predictions are mostly accurate for A_p^a values on the flexible
298 side. For buildings G2-3, G2-4 and G2-5, with 10, 13 and 15 stories, respectively, A_p^a values
299 at the lower third of the buildings are slightly underestimated (by a maximum value of 17%)
300 compared with the FE results. In order to prevent any damage in these cases, it is suggested
301 that the design of NSCs is performed using A_p^a values at $z/H = 1.0$. As illustrated in Fig. 5, the
302 predictions of the proposed model provides an upper bound on A_p^a values for the NSCs with
303 T_C equal to T_1 . For the NSCs with periods equal to the torsional fundamental period of the P-
304 structure (i.e., $T_C = T_3$), as depicted in Fig. 6, the predictions for the flexible sides are mainly
305 accurate, especially at upper floors, whereas for the NSCs at the centre of rigidity, a
306 conservative outcome is observed.



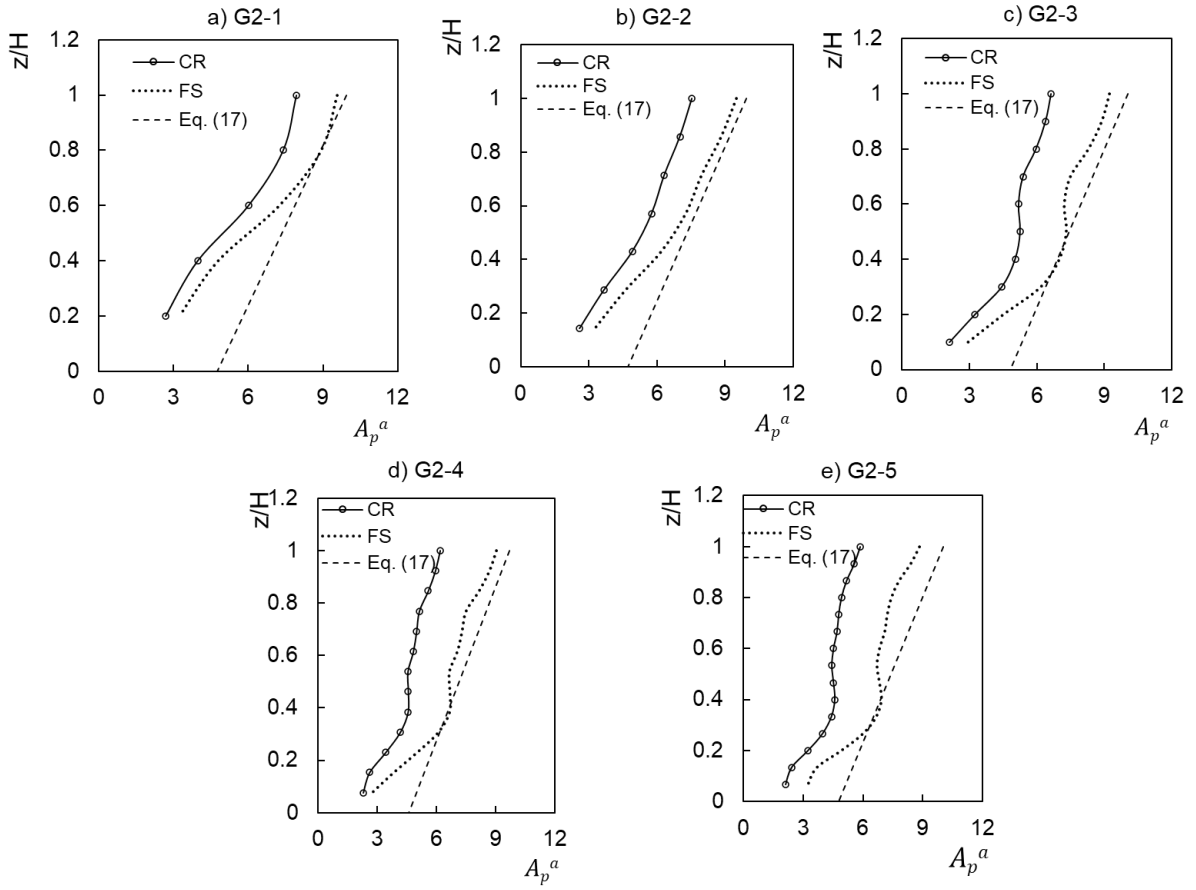
307

308

Fig. 4: Comparison between FE-predicted acceleration amplification factors (A_p^a) and predictions of Eq. (17) for rigid NSCs ($T_C \approx 0$ s)

309

310



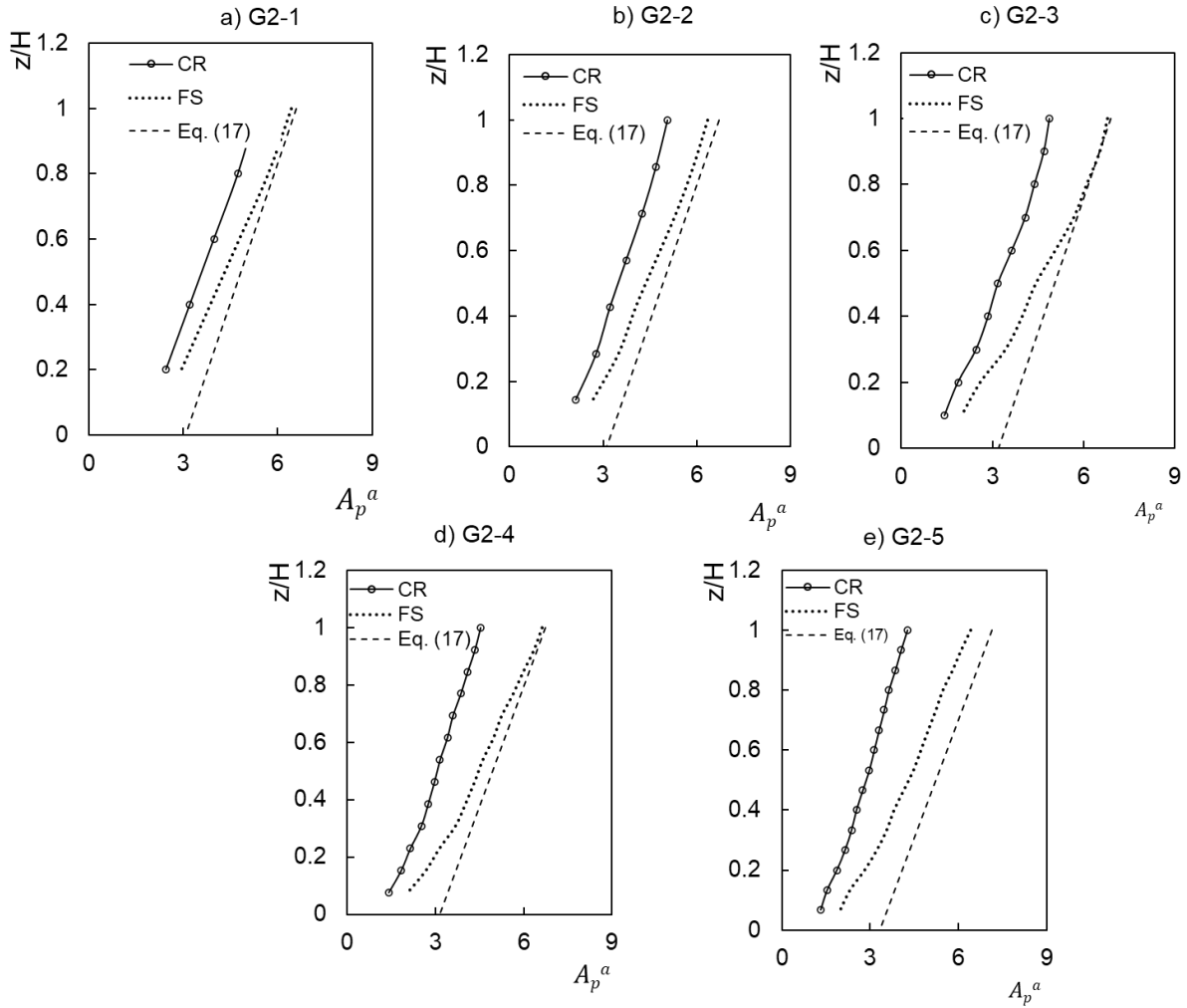
311

312

Fig. 5: Comparison between FE-predicted acceleration amplification factors (A_p^a) and

313

predictions of Eq. (17) for NSCs with $T_C=T_I$



314

315 Fig. 6: Comparison between FE-predicted acceleration amplification factors (A_p^a) and

316

predictions of Eq. (17) for NSCs with $T_C=T_3$

317

318

319

320

321

322

323

324

325

326

327

Table 2 shows the comparison between EC8 (2004) and Eq. (17) predictions for the NSCs with $T_C = T_I$ and attached to the flexible side of the top floors of G2 buildings. To demonstrate the improved safety offered by the proposed model over that offered by EC8 (2004) model, the predictions of the two design models are compared with the NSCs acceleration results at PGA values corresponding to the maximum seismic capacities of G2 buildings. Table 2 shows that, for the considered NSCs, EC8 (2004) underestimates the peak acceleration response by 50% on average. On the contrary, Eq. (17) offers improved performance and the predictions of the NSCs peak accelerations are improved by 41% on average (i.e., an average analytical-to-FE ratio of 91%). Overall, Figs. 4-6 and Table 2 demonstrate clearly the suitability of Eq. (17) for predicting the seismic response of NSCs attached to irregular RC P-structures with different heights.

328 Table 2: Comparison between EC8 (2004) and Eq. (17) predictions for NSCs with $T_C = T_I$
 329 and attached to the top floors of irregular RC buildings with different heights.

Building	PCA_{xy}	S_a (EC8)	S_a (Eq. (17))	S_a (EC8)	S_a (Eq. (17))
	(FEA) [g]	[g]	[g]	PCA_{xy} (FEA)	PCA_{xy} (FEA)
G2-1	3.17	1.58	2.89	0.50	0.91
G2-2	3.05	1.58	2.86	0.52	0.94
G2-3	3.20	1.58	2.88	0.49	0.90
G2-4	3.10	1.58	2.78	0.51	0.90
G2-5	3.15	1.58	2.88	0.50	0.91
Average				0.50	0.91
Standard deviation				0.01	0.02

330

331 5.2. Effect of ground type

332 The effect of various ground types was also considered for the assessment of the proposed
 333 design model. This is based on the FE results of Group 3 where the effect of ground types A,
 334 B, D and E on the seismic response of NSCs attached to the flexible side of the top floors of
 335 G3 buildings was studied.

336 Table 3 shows the comparison between EC8 (2004) and Eq. (17) predictions for the NSCs
 337 with $T_C = T_I$ at PGA values corresponding to the maximum seismic capacities of G3 buildings.
 338 As can be seen in Table 3, Eq. (17) is much safer than EC8 (2004) model. Eq. (17)
 339 underestimates the peak acceleration response of the NSCs attached to the buildings on ground
 340 types A, B, and D by about 16%, 10%, and 13% on average, respectively. For ground type E,
 341 Eq. (17) overestimates the peak acceleration response by approximately 9% on average. On the
 342 contrary, EC8 (2004) model underestimates the peak response of the NSCs for the four
 343 investigated ground types by 39 to 45%. Overall, Eq. (17) has a mean predicted-to-FE ratio of
 344 0.93 and a standard deviation of 0.10 whereas EC8 (2004) has a corresponding values of 0.52
 345 and 0.05, respectively.

346

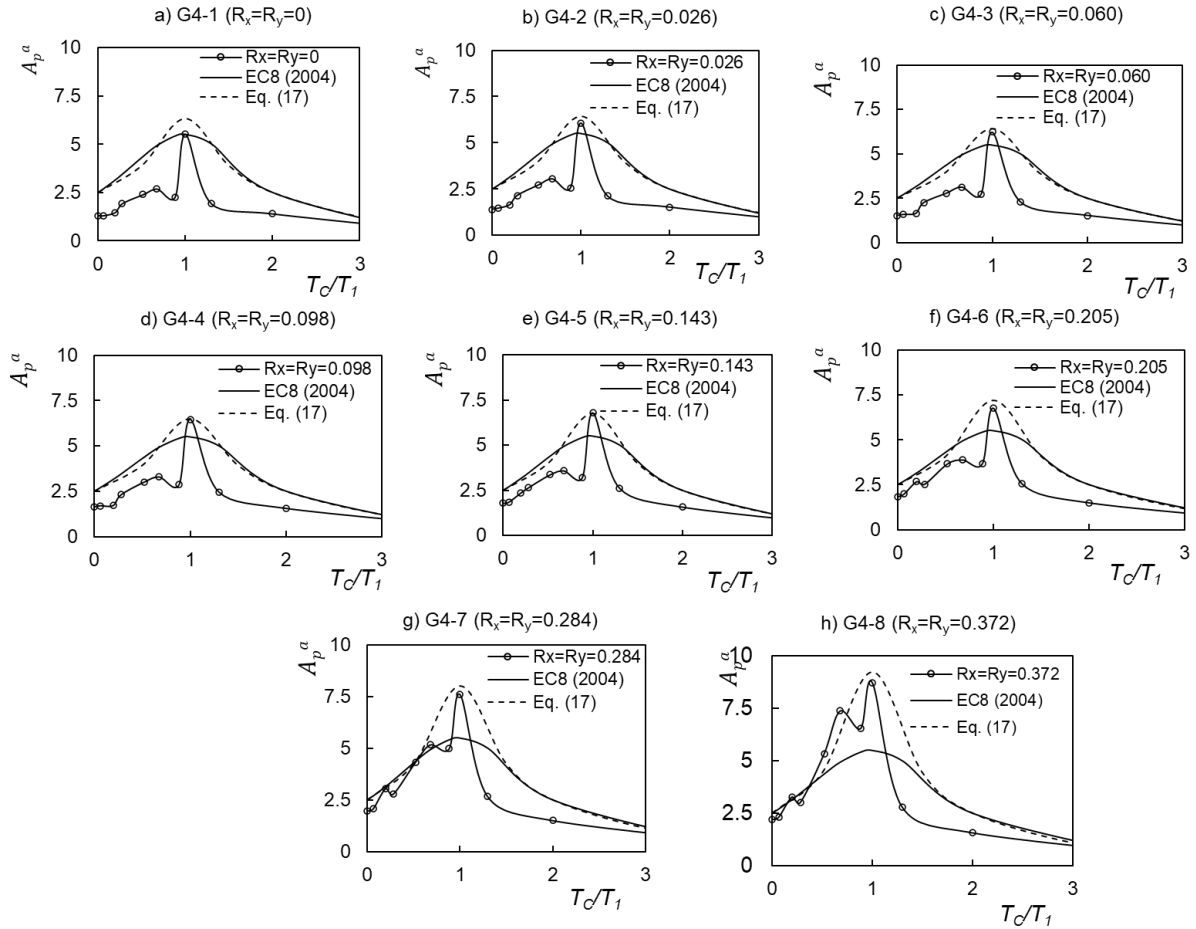
347 Table 3: Comparison between EC8 (2004) and Eq. (17) predictions for NSCs with $T_C = T_I$
 348 and attached to the top floors of irregular RC buildings on different ground types.

Building	PCA_{xy}	S_a (EC8)	S_a (Eq. (17))	S_a (EC8)	S_a (Eq. (17))
	(FEA) [g]	[g]	[g]	PCA_{xy} (FEA)	PCA_{xy} (FEA)
G3-1A	2.92	1.38	2.42	0.47	0.83
G3-1B	3.37	1.65	2.96	0.49	0.88
G3-1D	4.11	1.86	3.53	0.45	0.86
G3-1E	3.34	1.93	3.57	0.58	1.07
G3-2A	2.85	1.38	2.35	0.48	0.82
G3-2B	3.25	1.65	2.91	0.51	0.90
G3-2D	3.99	1.86	3.43	0.47	0.86
G3-2E	3.22	1.93	3.55	0.60	1.10
G3-3A	2.82	1.38	2.34	0.49	0.83
G3-3B	3.21	1.65	2.87	0.51	0.89
G3-3D	3.95	1.86	3.38	0.47	0.86
G3-3E	3.24	1.93	3.50	0.60	1.08
G3-4A	2.73	1.38	2.44	0.51	0.89
G3-4B	3.18	1.65	2.98	0.52	0.94
G3-4D	3.80	1.86	3.33	0.49	0.88
G3-4E	3.15	1.93	3.50	0.61	1.11
Average				0.52	0.93
Standard deviation				0.05	0.10

349 5.3. Effect of eccentricity ratio of the P-structure

350 Further to previous sections, the accuracy of the proposed model is herein assessed against
 351 the FE results of NSCs attached to RC buildings with different eccentricity ratios. Fig. 7
 352 presents the variation of A_p^a values on the flexible side (FS) of G4 buildings at PGA values
 353 corresponding to the elastic seismic capacities of the P-structures. Fig. 7 also compares the
 354 predictions of the proposed model and EC8 (2004) with the FE results. For G4-1 with $R_x = R_y$
 355 = 0 (i.e., regular building), both design models give safe predictions at $T_C = T_I$, with the
 356 proposed model overestimating the A_p^a value at $T_C = T_I$ by 14.9%. However, with increasing
 357 the eccentricity ratio from 0.026 (G4-2) to 0.372 (G4-8), EC8 (2004) model increasingly
 358 underestimates A_p^a values at $T_C = T_I$ from 9.4% (G4-2) to 36.9% (G4-8). Conversely, the
 359 proposed model gives consistently accurate predictions at $T_C = T_I$ for all irregular buildings,
 360 with a mean predicted-to-numerical ratio of 1.04 and a standard deviation of 0.03. As explained
 361 earlier in this paper, EC8 (2004) model does not take into consideration the effect of P-structure
 362 torsional behaviour and therefore underestimates the acceleration response of the NSCs
 363 attached to irregular buildings. On the other hand, the accurate predictions of Eq. (17) confirm
 364 that the proposed model adequately considers the effect of P-structure torsional behaviour.

365



366

367 Fig. 7: Comparison between acceleration amplification factors (A_p^a) and the predictions of
 368 Eq. (17) for NSCs attached to G4 buildings

369 6. Conclusions

370 This paper presents a new Eurocode-based model for the design of NSCs attached to
 371 irregular RC P-structures. The proposed model accounts for both the torsional behaviour and the
 372 maximum seismic capacity of an irregular RC P-structure. The new model is based on the
 373 results of more than 5000 nonlinear dynamic FEA of NSCs attached to irregular RC P-
 374 structures with different plan layouts, seismic capacities, total heights, ground types and
 375 eccentricity ratios. A subset of the FE results was used to calibrate the proposed model and
 376 another subset was used for model validation purposes.

377 Comparison between the FE results and EC8 (2004) predictions showed that, under tuned
 378 conditions, EC8 (2004) design model underestimates the acceleration response of NSCs on the
 379 flexible side of irregular RC P-structures. The gap between the FE results and EC8 (2004)
 380 predictions increased from 9.4 to 36.9% with increasing the eccentricity ratio from 0.026 to

381 0.372. On the other hand, the proposed design model has been demonstrated to be an
382 improvement over EC8 (2004) design provisions, particularly for NSCs on the flexible side
383 and in tune with the fundamental vibration period of the P-structure.

384 A parametric study was carried out to assess the effect of P-structure height, ground type,
385 and eccentricity ratio of the P-structure on the accuracy of the predictions of the proposed
386 model. For the vast majority of cases, the proposed model provided safe estimates for the
387 acceleration response of NSCs attached to different heights. For NSCs in tune with the
388 fundamental vibration periods of the P-structures, the proposed model accurately predicted the
389 variation of NSCs acceleration response with ground type or P-structure eccentricity ratio with
390 mean predicted ratios of 0.93 and 1.04, and standard deviations of 0.10 and 0.03, respectively.

391 **Declaration of competing interest**

392 The authors declare that they have no known competing financial interests or personal
393 relationships that could have appeared to influence the work reported in this paper.

394 **Acknowledgments**

395 The FE results presented in this paper were obtained using the University of Birmingham High
396 Performance Computing facility (BlueBEAR).

397 **References**

- 398 Agrawal, A.K. (1999), “Non-linear response of light equipment system in a torsional building
399 to bi directional ground excitation”, *Shock Vib.*, **6**(5), 223-236.
- 400 Agrawal, A.K. and Datta, T. (1999a), “Seismic behavior of a secondary system on a yielding
401 torsionally coupled primary system”, *J. Seismol. Earthq. Eng.*, **2**(1), 35-46.
- 402 Agrawal, A.K. and Datta, T. (1999b), “Seismic response of a secondary system attached to a
403 torsionally coupled primary system under bi-directional ground motion”, *J. Earthq. Technol.*
404 *- ISET*, **36**(1), 27-42.
- 405 Aldeka, A.B., Chan, A.H.C. and Dirar, S. (2014a), “Response of non-structural components
406 mounted on irregular RC buildings: comparison between FE and EC8 predictions”, *Earthq.*
407 *Struct.*, **6**(4), 351-373.
- 408 Aldeka, A.B., Dirar, S., Chan, A.H.C. and Martinez-Vazquez, P. (2015), “Seismic response of
409 non-structural components attached to reinforced concrete structures with different

410 eccentricity ratios”, *Earthq. Struct.*, **8**(5): 21pp.

411 Aldeka, A.B., Dirar, S., Martinez-Vazquez, P. and Chan, A.H.C. (2014b), “Influence of ground
412 type on the seismic response of non-structural components integrated on asymmetrical
413 reinforced concrete buildings”, In: *Proceedings of the Australian Earthquake Engineering
414 Society 2014 Conference*, Nov 21 -23, Lorne, Victoria, 11pp.

415 Anajafi, H. and Medina, R.A., 2018, June. Effects of Supporting Building Characteristics on
416 Nonstructural components Acceleration Demands. In 11th US National Conference on
417 Earthquake Engineering.

418 Anajafi, H. and Medina, R.A. (2019) Lessons learned from evaluating the responses of
419 instrumented buildings in the United States: The effects of supporting building
420 characteristics on floor response spectra. *Earthquake Spectra*, 35(1), pp.159-191.

421 ASCE (2010), *Minimum design loads for buildings and other structures*, American Society of
422 Civil Engineers, ASCE/SEI Standard 7-10, Reston, VA.

423 Chaudhuri, S.R. and Villaverde, R. (2008), “Effect of building nonlinearity on seismic response
424 of nonstructural components: a parametric study”, *J. Struct. Eng.*, ASCE, **134**(4), 661-670.

425 EC1 (2002), EN 1991-1-1 Eurocode 1, *Actions on structures, Part 1-1: General actions –
426 Densities, self-weight, imposed loads for buildings*, European Committee for Standardization,
427 Brussels, Belgium.

428 EC2 (2004), EN 1992-1-1 Eurocode 2, *Design of concrete structures, Part 1-1: General rules
429 and rules for buildings*, European Committee for Standardization, Brussels, Belgium.

430 EC8 (2004+A1:2013), EN 1998-1 Eurocode 8, *Design of structures for earthquake resistance,
431 Part 1: General rules, seismic actions and rules for buildings*, European Committee for
432 Standardization, Brussels, Belgium.

433 Fajfar, P. (2002). Structural analysis in earthquake engineering - a breakthrough of simplified
434 non-linear methods. In *Proceedings of the 12th European Conference on Earthquake
435 Engineering*, September 9-13, London, UK, 20pp.

436 Fajfar, P., Kilar, V., Marusic, D., Perus, I. and Magliulo, G. (2005a). The extension of the N2
437 method to asymmetric buildings. In *Proceedings of the 4th European Workshop on the
438 Seismic Behaviour of Irregular and Complex Structures*, August 26-27, Thessaloniki, Greece,
439 16pp.

440 Fajfar, P., Marušić, D. and Peruš, I. (2005b). Torsional effects in the pushover-based seismic
441 analysis of buildings. *Journal of Earthquake Engineering*, 9 (6): 831-854

442 Filiatrault, A. and Sullivan, T. (2014) “Performance-based seismic design of nonstructural

443 building components: The next frontier of earthquake engineering”. *Earthquake Engineering*
444 *and Engineering Vibration*, **13**(1), pp.17-46.

445 Gelfi, P. (2007), “SIMQKE_GR, Programma per la generazione di accelerogrammi artificiali
446 spettro-compatibili”, Italy: University of Brescia.

447 Graves, H. and Morante, R. (2006), *Recommendations for revision of seismic damping values*
448 *in Regulatory Guide 1.61*, U.S. Nuclear Regulatory Commission, Office of Nuclear
449 Regulatory Research, Washington.

450 Iervolino, I., Galasso, C. and Cosenza, E. (2010), “REXEL: computer aided record selection
451 for code-based seismic structural analysis”, *Bull. Earthq. Eng.*, **8**(2), 339-362.

452 Johnson, T.P., Dowell, R.K. and Silva, J.F. (2016) “A review of code seismic demands for
453 anchorage of nonstructural components” *Journal of Building Engineering*, **5**, pp.249-253.

454 Kreslin, M. and Fajfar, P. (2010). Seismic evaluation of an existing complex RC building.
455 *Bulletin of Earthquake Engineering*, 8 (2): 363-385

456 Lim, Ellys, Lizhong Jiang, and Nawawi Chouw. “Dynamic response of a non-structural
457 component with three supports in multi-directional earthquakes.” *Engineering Structures*
458 **150** (2017): 143-152.

459 Lima, C. and Martinelli, E. (2019) “Seismic Response of Acceleration-Sensitive Non-
460 Structural Components in Buildings”. *Buildings*, **9**(1), p.7.

461 Mander, J., Priestley, M.N. and Park, R. (1988), “Theoretical stress-strain model for confined
462 concrete”, *J. Struct. Eng.*, ASCE, **114**(8), 1804-1826.

463 Martinelli, E. and Faella, C. (2016) “An overview of the current code provisions on the seismic
464 response of acceleration-sensitive non-structural components in buildings” In *Applied*
465 *Mechanics and Materials*. **847**, 273-280. Trans Tech Publications Ltd.

466 McKevitt, W. (2004), “Reply to the discussion by RD Watts on Proposed Canadian code
467 provisions for seismic design of elements of structures, nonstructural components, and
468 equipment”, *Canadian J of Civil Eng.*, **31**(2), 392-392.

469 Menegotto, M. and Pinto, P.E. (1973), “Method of analysis for cyclically loaded RC plane
470 frames including changes in geometry and non-elastic behaviour of elements under
471 combined normal force and bending”, *Symposium on the Resistance and Ultimate*
472 *Deformability of Structures acted on by well defined loads*, International Association for
473 Bridge and Structural Engineering, Zurich, Switzerland.

474 MIDAS Gen (2012), *Analysis manual*, version 2.1, <http://www.MidasUser.com/>.

475 Mohammed, H.H., Ghobarah, A. and Aziz, T.S. (2008), “Seismic response of secondary

476 systems supported by torsionally yielding structures”, *J. Earthq. Eng.*, **12**(6), 932-952.

477 Mohsenian, V., Gharaei-Moghaddam, N. and Hajirasouliha, I. (2019) “Multilevel seismic
478 demand prediction for acceleration-sensitive non-structural components” *Engineering
479 Structures*, **200**, p.109713.

480 Negro, P., Mola E., Molina F.J. and Magonette G.E. (2004), “Full-scale PSD testing of a
481 torsionally unbalanced three-storey non-seismic RC frame”, In: *Proceedings of 13th World
482 conference on Earthquake Engineering*, Vancouver, Canada, No. 968.

483 Oropeza, M., Favez, P. and Lestuzzi, P. (2010), “Seismic response of nonstructural
484 components in case of nonlinear structures based on floor response spectra method”, *Bull.
485 Earthq. Eng.*, **8**(2), 387-400.

486 Petrone, C., Magliulo, G. and Manfredi, G. (2015) “Seismic demand on light acceleration-
487 sensitive nonstructural components in European reinforced concrete buildings” *Earthquake
488 engineering & Structural dynamics*, **44**(8), pp.1203-1217.

489 Rozman, M. and Fajfar, P. (2009), “Seismic response of a RC frame building designed
490 according to old and modern practices”, *Bull Earthq. Eng.*, **7**(3): 779-799.

491 Sackman, J.L. and Kelly, J.M. (1979), “Seismic analysis of internal equipment and components
492 in structures”, *Eng. Struct.*, **1**(4), 179-190.

493 Sousa, L. and Monteiro, R. (2018) “Seismic retrofit options for non-structural building partition
494 walls: Impact on loss estimation and cost-benefit analysis” *Engineering structures*, **161**,
495 pp.8-27.

496 Stefano, D. M. and Pintucchi, B. (2010). Predicting torsion-induced lateral displacements for
497 pushover analysis: Influence of torsional system characteristics. *Earthquake Engineering
498 & Structural Dynamics*, **39** (12): 1369-1394.

499 Surana M, Singh Y, Lang DH. (2018) Effect of irregular structural configuration on floor
500 acceleration demand in hill-side buildings. *Earthquake Engng Struct Dyn.*;1–23

501 UBC (2012), *International Conference of Building Officials*, Uniform Building Code. Whittier,
502 California, USA.

503 Yang, Y.B. and Huang, W.H. (1993), “Seismic response of light equipment in torsional
504 buildings”, *Earthq. Eng. Struct. Dyn.*, **22**(2), 113-128.

505 Yang, Y.B. and Huang, W.H. (1998), “Equipment–structure interaction considering the effect
506 of torsion and base isolation”, *Earthq. Eng. Struct. Dyn.*, **27**(2), 155-171